Journal of Orthopaedic Surgery and Research

RESEARCH

Open Access

Age-related traumatic anatomy and personalized medial incision design for calcaneal fractures in older adults using three-dimensional mapping

Yuanzhen Zhang[1†], Jiayun Liu[1†], Jinhua Yang[1], Ye Yuan[3], Guoyong Yin[1*], Yu Zhang[1*] and Chun Lu[2*]

Abstract

Background Calcaneal fractures usually arise from high-energy trauma and predominantly impact young individuals. In older adults (aged ≥ 50 years), declining bone density and muscle strength increase fracture risk from low-energy trauma, leading to a bimodal epidemiological distribution. The intricacies of calcaneal fractures in older adults, alongside osteoporosis and soft tissue fragility, complicate surgical intervention. This study aims to analyze age-related differences in calcaneal fracture characteristics using three-dimensional(3D) mapping and assess their impact on medial incision design.

Method A total of 95 patients with closed calcaneal fractures were categorized into two groups: Younger (< 50 years, $n = 61$) and Older (≥ 50 years, $n = 34$). The process of 3D fracture mapping was executed utilizing Mimics and 3-matic software, alongside the reconstruction of soft tissue, which encompassed the posterior tibial neurovascular bundle. Differences in fracture distribution and incision parameters (length, α angle, D1, and D2) were statistically analyzed, with $p < 0.05$ considered statistically significant.

Results Fracture lines in both groups were predominantly located around the lateral Gissane's angle and critical weight-bearing areas of the calcaneus. In the Younger Group, fracture lines were long, continuous, and involved fewer fragments, correlating with high-energy trauma. The Older Group showed more comminuted lines, characteristic of osteoporotic fractures. The α angle and D1 distance were significantly smaller in the Older Group ($p < 0.05$), indicating closer proximity to the medial malleolus. D2 values were also smaller ($p < 0.05$), with 48.65% intersecting the neurovascular bundle compared to 31.34% in the Younger Group.

†Yuanzhen Zhang and Jiayun Liu contributed equally to this work.

*Correspondence:
Guoyong Yin
yinguoyongortho@163.com
Yu Zhang
zhangyuortho@gmail.com
Chun Lu
luchun_njmu@163.com

Full list of author information is available at the end of the article

Conclusion Age significantly influences medial wall fracture patterns and complexity in calcaneal injuries. A personalized medial incision based on fracture morphology provides better exposure and reduction compared to traditional methods. Although the incision is closer to the neurovascular bundle in older patients, meticulous surgical technique guarantees safety. The integration of a medial incision with sinus-tarsi (ST) approach minimizes the necessity for extensive lateral exposure, thereby diminishing soft tissue complications and improving surgical outcomes for the elderly population.

Level of evidence Level IV, retrospective case series.

Keywords Calcaneal fractures, Medial wall fracture, Older adults, Osteoporosis, Three-dimensional mapping

Background

Calcaneal fractures frequently occur in clinical settings. High-energy trauma primarily results in these fractures among young adults aged 20 to 40. In contrast, older adults over 50 experience similar fractures due to age-related declines in bone density and muscle strength, often from low-energy injuries [1, 2]. This creates a bimodal epidemiological distribution [3–5]. However, most research have focused on younger patients, leaving a gap in our understanding of fracture management in older persons, who face extra hurdles from osteoporosis, diminished bone strength, and impaired soft tissue due to comorbidities [6, 7]. While discussions persist concerning surgical intervention, evidence suggests that properly managed displaced intra-articular fractures in older patients can lead to positive outcomes [8, 9].

Incision design is particularly critical in older patients because fragile skin increases the risk of necrosis [10]. The extensile L (EL) lateral incision provides broad visualization of the subtalar and calcaneocuboid joints and facilitates correction of deformity; however, its large skin flap and extensive soft-tissue dissection are associated with a 15–25% wound-complication rate [11–13]. By contrast, the sinus-tarsi (ST) approach is considerably less invasive and has a much lower incidence of wound problems, yet it affords only limited restoration of calcaneal length and varus alignment [13–15]. Accordingly, in elderly patients—especially those with highly comminuted medial-wall fractures—a supplementary, patient-specific medial incision is often necessary to achieve satisfactory reduction while safeguarding the soft tissues.

The medial approach for treating calcaneal fractures was first proposed by McReynolds in 1953 [16]. Burdeaux and Stephenson later introduced variations of medial calcaneal incisions [17, 18]. These incisions aim to fully expose the fractured medial wall and restore calcaneal length and height through precise reduction. This method facilitates access to the collapsed subtalar joint fragments, enabling their reduction and fixation through a limited lateral incision, thereby circumventing the need for a more extensive L-shaped incision. While different medial approaches vary in exposure range and proximity to the posterior tibial neurovascular bundle, they all seek to follow paths near the main fracture line while protecting critical neurovascular structures [19, 20]. Nonetheless, the existing body of research on the traumatic anatomy of medial calcaneal fractures in older adults is insufficient, leaving unresolved questions about fracture distribution and optimal incision design. This gap hinders the advancement of tailored surgical strategies that integrate medial and limited lateral approaches [21].

Using 3D mapping, this study analyzes age-related fracture line distribution and its impact on medial incision design, providing evidence for combined medial and limited lateral incisions.

Method

Subjects

This study was approved by the Ethics Committee of the First Affiliated Hospital of Nanjing Medical University. Inclusion criteria included: [1] patient age ≥ 18 years; [2] availability of complete original CT scan data suitable for 3D reconstruction and surgical simulation; and [3] presence of a closed calcaneal fracture. The exclusion criteria included: [1] patients under 18 years of age; [2] pathological fractures; [3] history of previous surgery at the fracture site; [4] open fractures; [5] comminuted fractures with unclear fracture lines; and [6] Sanders type I fractures, as these fractures typically exhibit minimal displacement and are generally managed with conservative treatment.

Calcaneal bone reconstruction and fracture line mapping

All patients underwent CT scans (Siemens, Berlin, Germany), with the resultant data archived in Digital Imaging and Communication in Medicine (DICOM) format. These DICOM data were imported into Mimics Research 21.0 software (Materialise, Leuven, Belgium) to generate 3D models of the calcaneus, which were used for subsequent measurements (Fig. 1A-B). The 3D models of the calcaneal fractures were then imported into 3-matic Research 13.0 software (Materialise, Leuven, Belgium). The standard model used for comparison was based on the right calcaneus; therefore, all left calcaneal models were mirrored to match the right side (Fig. 1C). Within 3-matic, the fracture models were aligned with the

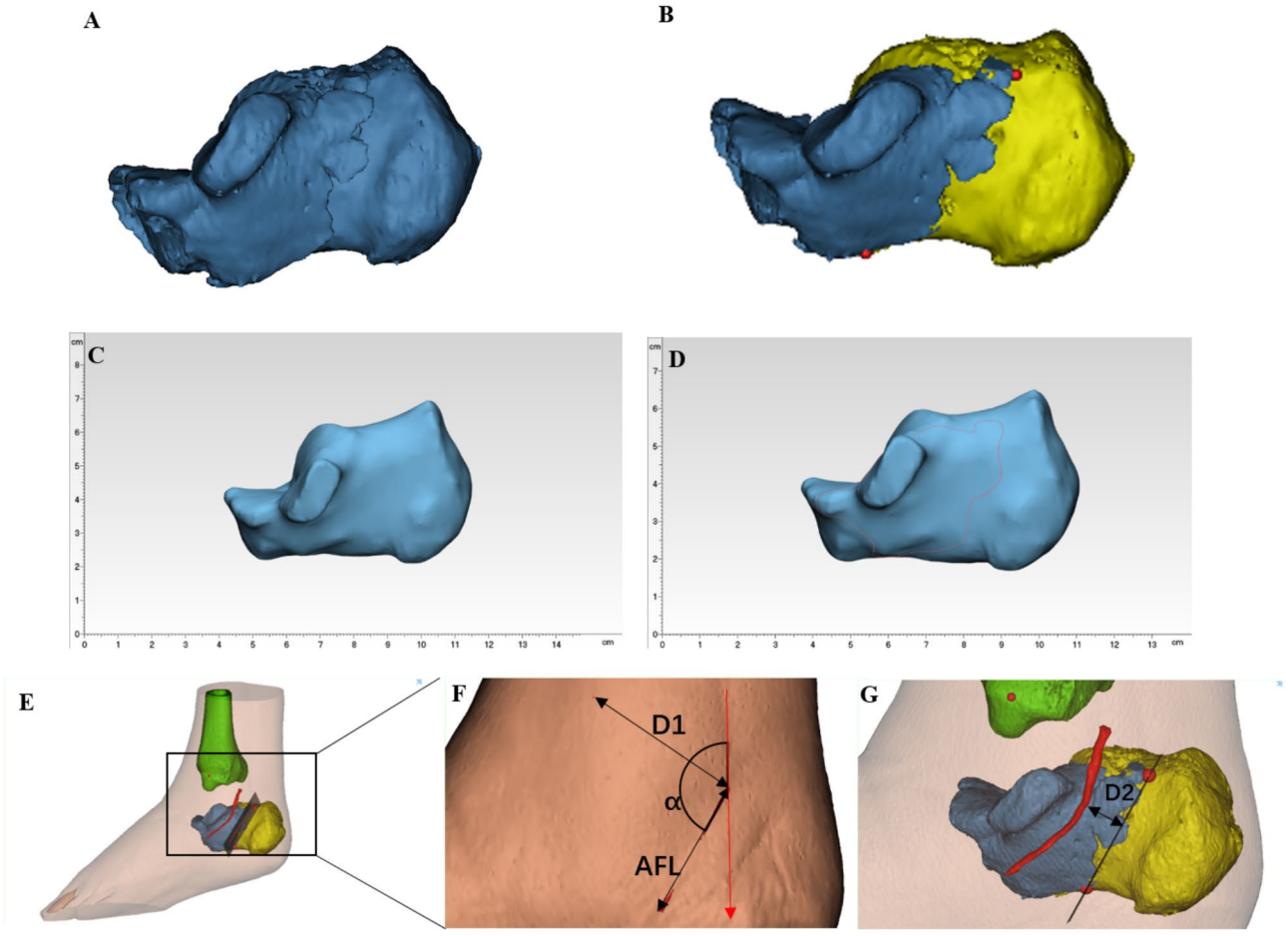

Fig. 1 Comprehensive 3D mapping -Based Strategy for Calcaneal Fracture Mapping and Personalized Medial Incision Design. (**A**) 3D reconstruction of the fractured calcaneus using Mimics Research 21.0®. (**B**) Fragment reduction and alignment performed in 3-matic Research 13.0®. (**C**) Standardized calcaneus template model. (**D**) Fracture lines depicted in red on the standardized template. (**E**) 3D reconstruction of the distal tibia, calcaneus, and posterior tibial neurovascular bundle. A visual plane was established through the abstracted fracture line (AFL) and vertically intersected the medial soft tissue surface. (**F**, **G**) Point A indicates the tip of the medial malleolus, and the red line represents the tibial axis. D1 is the shortest distance from the medial malleolus to the AFL; α is the angle between the AFL and the tibial axis; and D2 is the shortest distance from the AFL to the neurovascular bundle

standard model using the "N points registration" function, ensuring both were positioned identically in the same spatial orientation. The fracture lines were then traced and mapped directly onto the standardized model (Fig. 1D).

To investigate the differences in fracture patterns between different age groups, patients were divided into two groups: Older Group (aged 50 years and above) and Younger Group (aged below 50 years). Separate 3D fracture mapping diagrams were created for each group, enabling a qualitative comparison of fracture distribution between the two. The resulting diagrams were saved as TXT files, with coordinates recorded to an accuracy of 0.0001 mm, expressed in (x, y, z) format. The fracture lines were then converted into 3D heat maps using the E-3D Digital Medical Platform® (Central South University, Changsha, China). These heat maps were generated based on the frequency of fracture line occurrence at each location, with a 5 mm buffer distance applied to account for minor tracing errors and anatomical variations. Distance weighting was applied during the calculations to enhance accuracy.

Soft tissue reconstruction and medial incision design and measurement

Based on the reconstructed calcaneal fracture models, Mimics software was used to reconstruct the soft tissue of the foot and the posterior tibial neurovascular bundle, allowing for easier subsequent measurements. The proximal and distal endpoints of the primary fracture line were connected to form an abstracted fracture line (AFL), representing the length of the fracture line. The perpendicular projection of this line onto the surface of the medial soft tissue model of the heel was defined as the idealized virtual surgical incision (Fig. 1E). For all samples, the following measurements were taken: [1] the

length of the AFL (L), representing the shortest length of the medial incision; [2] the shortest distance from the tip of the medial malleolus to the AFL (D1); [3] the angle (α) between the AFL and the anatomical axis of the tibia (Fig. 1F); and [4] a virtual cross-sectional plane through the AFL, perpendicular to the medial soft tissue, was established to represent the deep anatomical path. The minimum distance from this plane to the posterior tibial artery, vein, and nerve bundle was recorded as D2 (Fig. 1G).

Statistical analysis

Data were analyzed utilizing Statistical Product and Service Solutions (SPSS) software version 20.0 (IBM, Inc., Armonk, NY, USA). Continuous variables were expressed as mean ± standard deviation (SD), while categorical data were presented as frequencies and percentages. Independent-samples t-tests were applied to normally distributed data, whereas the Mann-Whitney U test was used for non-normally distributed data to compare differences in incision parameters (L, α, D1, and D2) between the younger and older patient groups. Data normality was assessed before applying independent t-tests or Mann-Whitney U tests as appropriate. A *p*-value of less than 0.05 was considered statistically significant.

Results

Demographic and clinical characteristics of the patients

Patient data for this study were collected between January 2010 and December 2022, and 95 patients with closed calcaneal fractures were included. Out of these, 61 patients were identified in the Younger Group (under 50 years), while the Older Group (50 years and above) comprised 34 patients. Table 1 presents the data for the two groups of cases. A total of 104 calcaneal fracture cases were analyzed, including 9 patients with bilateral calcaneal fractures. The mean age of the Younger Group was 38.66 ± 8.02 years, whereas the mean age of the Older Group was 55.74 ± 9.16 years, with a statistically significant difference between the two groups ($p < 0.001$). The gender distribution between the two groups showed no statistically significant difference ($p = 0.824$). The analysis of fracture occurrence revealed that the distribution of left and right calcaneal fractures was comparable between the two groups, showing no statistically significant difference ($p = 0.839$). Fracture types were classified according to the Sanders classification. The results showed that Sanders type II fractures were predominant in the Younger Group (47.8%), while Sanders type III and IV fractures were more common in the Older Group (43.2% and 35.1%, respectively). The difference in the distribution of Sanders classifications between the two groups was statistically significant ($p = 0.008$). All patients had a complete set of original CT scans, which were used for 3D reconstruction and surgical simulation.

Comparison of fracture line distribution between the younger and older groups

In the Younger Group ($n = 67$), fracture lines were mainly concentrated in the lateral Gissane's angle, posterior region, and weight-bearing areas of the calcaneus. The fracture lines had clear orientations and were associated with fewer fracture fragments, most of which were long and continuous, consistent with injury patterns typically seen after high-energy trauma; however, a direct causal relationship cannot be confirmed. External forces were transmitted through the lateral calcaneus, leading to more concentrated fractures. The fracture lines on the medial wall were relatively concentrated and ran below the sustentaculum tali in a direction from the posterior superior to the anterior inferior region. Several additional fracture lines were noted in various orientations, with some intersecting the surface of the sustentaculum tali (Fig. 2A-F).

Table 1 Demographic and clinical characteristics of patients

	Total ($n = 95$ Patients, $n = 104$ Cases)	Younger Group ($n = 67$ Cases)	Older Group ($n = 37$ Cases)	*p* value
Age, mean ± SD	44.77 ± 11.76	38.66 ± 8.02	55.74 ± 9.16	< 0.001
Sex, n(%)				0.824
Male	79(83.2)	50 (82.00)	29 (85.29)	
Female	16(16.8)	11 (18.00)	5 (14.71)	
Side of injury, n(%)				0.839
Left	36(34.62)	28 (41.79)	17 (45.95)	
Right	68(65.38)	39 (58.21)	20 (54.05)	
Subtypes, n(%)				0.008
Sanders II	44(42.31)	32 (47.76)	8 (21.62)	
Sanders III	39(37.50)	26 (38.81)	16 (43.24)	
Sanders IV	21(20.19)	9 (13.43)	13 (35.14)	

Note:Age and sex variables are based on the number of patients ($n = 95$), while side of injury and fracture subtypes are based on the number of fracture cases ($n = 104$), as some patients had bilateral fractures. *p*-values for continuous variables (e.g., age) are calculated using the independent-samples t-test, while *p*-values for categorical variables (e.g., sex, side of injury, and fracture subtypes) are calculated using the Chi-square test. Statistical significance is indicated by $p < 0.05$

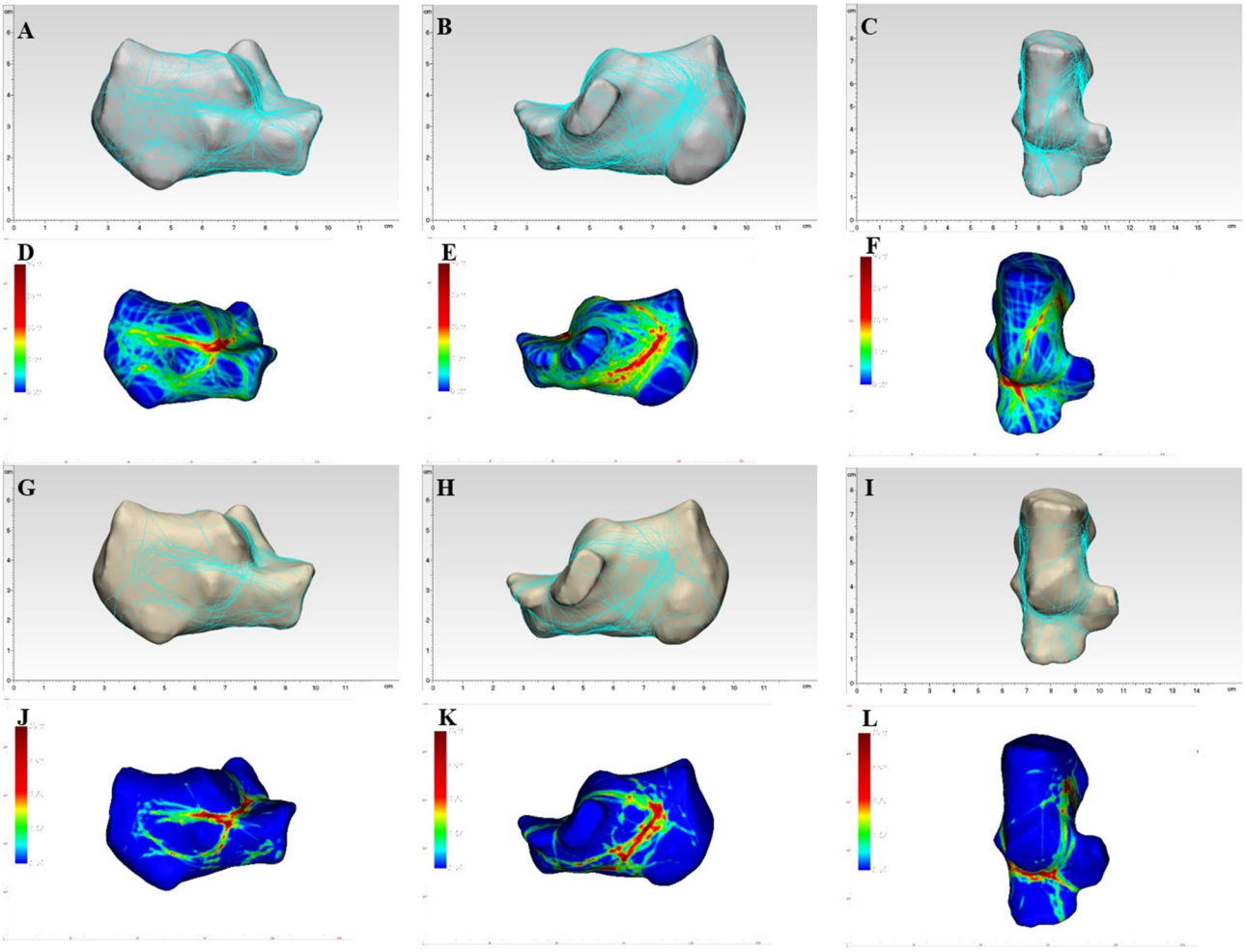

Fig. 2 Comparison of Calcaneal Fracture Line Distributions and 3D Heat Maps in Younger and Older Groups. (**A**–**C**) Younger Group. Lateral (**A**), medial (**B**), and superior (**C**) views of fracture lines superimposed on the standardized calcaneus template. A 3D heat map (**D**–**F**) illustrates fracture frequency and severity, with darker colors indicating higher occurrence rates in the respective regions. (**G**–**I**) Older Group. Lateral (**G**), medial (**H**), and superior (**I**) views of fracture lines similarly mapped onto the calcaneus template. Again, a 3D heat map (**J**–**L**) denotes regions of elevated fracture frequency and severity, shown by darker color gradients

In the Older Group ($n = 37$), fracture lines were mainly distributed in the lateral Gissane's angle, the subtalar joint surface, and below the medial sustentaculum tali, with a more scattered distribution in the plantar region. The fracture lines displayed a closer proximity, demonstrated multidirectional patterns, and were linked to a greater number of fragmented segments, illustrating the defining features of osteoporotic fractures characterized by multiple fragments. The fracture lines on the medial wall were oriented similarly to those in younger patients, running below the sustentaculum tali from the posterior superior to the anterior inferior region. However, compared to younger patients, the primary fracture lines were closer to the sustentaculum tali. Multiple primary fracture lines were observed in the medial wall near the plantar region (Fig. 2G-L).

Comparison of incision parameters between the younger and older groups

The comparison of incision-related parameters between the two groups is presented in the Table 2. The length of the incision (L) was similar between the two groups, with values of 40.04 ± 6.65 mm in the Younger Group and 40.68 ± 8.82 mm in the Older Group, and the difference was not statistically significant. There were significant differences in D1 and α between the two groups (38.75 (11.26) vs. 34.29 (13.45); 144.15 (19.37) vs. 135.24 (19.55), respectively) ($p < 0.05$). The D2 value, which represents the shortest distance between the incision plane and the posterior tibial neurovascular bundle, was significantly smaller in the Older Group compared to the Younger Group (5.15 (9.15) vs. 2.45 (5.72); $p < 0.05$). In the Younger Group, 21 cases (31.34%) had the incision plane intersecting with the posterior tibial neurovascular bundle

Table 2 Comparison of incision parameters (L, D1, A, and D2) between younger and older groups

Variables	Younger Group ($n=67$)	Older Group ($n=37$)	t/U	*p* value
L(mm)	40.04 ± 6.65	40.68 ± 8.82	0.130	0.897
D1(mm)	38.75 (11.26)	34.29 (13.45)	1699.0	0.002
α(°)	144.15 (19.37)	135.24 (19.55)	1675.5	0.003
D2(mm)	5.15 (9.15)	2.45 (5.72)	1521.0	0.025

Note:Continuous variables are presented as Mean ± SD for normally distributed data or Median (IQR) for non-normally distributed data. Normality was assessed using the Shapiro-Wilk test. For normally distributed variables, an independent-samples t-test was used to compare means between groups. For non-normally distributed variables, the Mann-Whitney U test was used. Statistical significance is indicated by $p<0.05$

(D2 = 0), whereas in the Older Group, 18 cases (48.65%) showed such intersection. The difference between the two groups was not statistically significant ($p=0.0717$).

Discussion

While calcaneal fractures have been extensively researched, the age-related variations warrant further investigation. This study is the first to use 3D mapping technology to assess age-related changes in calcaneal fracture anatomy and its implications for medial calcaneal incisions. In both Younger and Older Groups, fracture lines clustered in weight-bearing zones near Gissane's angle, radiating toward the lateral wall. Fractures of the medial wall extended from the posterior superior to the anterior inferior regions. These distribution patterns are broadly consistent with earlier fracture-mapping reports [22, 23], supporting the external validity of our dataset. In younger patients, these fractures presented as long, continuous lines, whereas older individuals exhibited fragmented, multidirectional patterns, indicative of diminished bone quality and heightened fracture complexity.

Focusing on medial wall fractures is important for two key reasons: [1] The medial wall's thicker cortex and proximity to the lower-extremity weight-bearing axis provide critical support, making its injury indicative of overall calcaneal damage [24] [2]. Inadequate restoration risks calcaneal tuberosity varus, shortening, and proximal migration, leading to persistent biomechanical issues despite reduced subtalar joint disruption [25]. Therefore, medial wall reduction is a central treatment goal.

This research revealed notable disparities in the distribution of medial wall fracture lines between the Younger and Older Groups, which have direct implications for surgical approaches. In younger patients, fracture lines were more concentrated, often crossing the surface of the sustentaculum tali and indicating larger bone fragments farther from it. These fractures tend to occur in areas of thinned cortical bone. Shi et al. also noted that fractures in younger patients were more directed and less fragmented [26], and can typically be reduced effectively through lateral incisions or medial distractors, without requiring direct medial incision visualization [11, 27]. The postoperative X-ray images presented in Fig. 3A and B illustrate that, in the Younger Group, fractures—despite displacement—are more readily aligned via lateral incisions, resulting in the medial wall being restored to a functional position. This is consistent with the observed pattern of more concentrated and less fragmented fractures, which can be managed effectively with minimally invasive lateral approaches.

In contrast, fractures of the medial wall in the Older Group were more complex, typically closer to the sustentaculum tali, and involved smaller bone fragments. Secondary fracture lines led to further comminution, complicating reduction via a single lateral incision. With the progressive decline in bone strength associated with aging, fractures tend to become increasingly comminuted, impacting a broader area of the medial wall and complicating the surgical reduction process. These findings align with those of Guha et al., who showed that fractures in older patients are more complex due to osteoporosis-related bone weakness [28]. In a similar vein, Guo et al. observed that fractures in older patients exhibited a more extensive distribution, especially in the lateral, posterior, and articular areas of the calcaneus. This was characterized by narrower intervals between fracture lines, leading to heightened fragmentation and greater difficulty in achieving reduction [29]. This complexity is clearly visible in the postoperative X-ray images from the Older Group (Fig. 3C and D), where despite the use of the same lateral incision approach, the medial wall remains misaligned and displaced, illustrating the limitations of this technique in more fragmented fractures. Severe medial wall damage presents three key challenges: first, comminution compromises the medial column, requiring robust internal fixation [24, 30], as locking lateral plating may be insufficient, while medial column screws risk loss of reduction due to a thick, fragmented cortex [31, 32]. Second, comminution complicates indirect reduction approaches [27]. Third, small sustentaculum tali fragments reduce screw-holding power [33]. These challenges, as highlighted by the poor alignment shown in Fig. 3, underscore the need for additional medial approaches. Incomplete medial wall restoration correlates with poor outcomes [34], and a medial incision can enhance fracture reduction and restore calcaneal height and length [35].

It is essential to prevent harm to the posterior tibial neurovascular bundle [21, 36]. After three-dimensional

Fig. 3 Postoperative X-ray Images of Calcaneal Fractures in Younger and Older Groups. (**A**–**B**) Younger Group. Postoperative anteroposterior (**A**) and axial (**B**) X-ray images of the calcaneal fracture showing fracture alignment and fixation. (**C**–**D**) Older Group. Postoperative anteroposterior (**C**) and axial (**D**) X-ray images of the calcaneal fracture demonstrating fracture reduction and hardware positioning

reconstruction, we derived an individualized virtual incision plane by orthogonally projecting the abstract fracture line (AFL) onto the medial skin. In most case this plane lay posterior to the tarsal tunnel—an area in which neurovascular branching is sparse, whereas most divisions arise anterior-distally [21, 37]. Although in a subset of specimens the plane intersected or abutted the bundle (D2 = 0), the intact tunnel can be gently mobilized anteriorly; entering through this posterior corridor therefore obviates intra tunnel dissection and markedly reduces neurovascular risk. In addition, the mean simulated incision length (~ 40 mm) is substantially shorter than traditional medial cuts [17, 18], which—together with systematic pre-operative 3D mapping evaluation—helps

limit soft-tissue stripping and the propensity for hypertrophic scarring [38].

Finally, we emphasize that the present work represents an imaging-based modelling exploration; ethical approval for a prospective clinical study is in progress, and the personalized incision has not yet been applied in patients. Together with the limited number of older participants, reliance on imaging rather than functional outcomes, and omission of patient-specific factors such as BMI and bone-mineral density, this may restrict the generalizability of our conclusions. Future work that integrates these variables with clinical follow-up data should help to refine and validate the proposed incision design.

Conclusion

This research, utilizing advanced 3D mapping technology, demonstrated that age plays a crucial role in the intricacy of medial wall fractures associated with calcaneal injuries, thereby posing more significant treatment challenges for older adults. Personalized medial incisions based on the morphology of the primary fracture lines provide better exposure of medial wall fractures compared to classical medial approaches. Although such incisions are closer to the posterior tibial neurovascular bundle, proper handling during surgery can achieve safe and effective reduction. The incorporation of a medial incision combined with sinus-tarsi (ST) approach can effectively reduce the need for an extended lateral approach, thereby minimizing soft tissue complications and enhancing surgical safety in older adult patients.

Acknowledgements
We are grateful to all participants and their families enrolled in this study. We thank for the support of the nursing staffs from the department of orthopaedic of The First Affiliated Hospital with Nanjing Medical University.

Author contributions
Y.Z. and J.L. contributed equally to this work as co-first authors. Y.Z. and J.L. designed the study, performed data analysis, interpreted results, and wrote the main manuscript text. J.Y. and Y.Y. contributed to patient data collection and image processing. G.Y., Y.Z. and C.L.(corresponding author) supervised the research design, critically reviewed the manuscript, and provided revisions and guidance throughout the study. All authors have read, revised, and approved the final manuscript for publication.

Funding
The authors acknowledge financial support from the National Natural Science Foundation of China (Grant Nos. 82372408, 82472427, 82030069), the Natural Science Foundation of Jiangsu Province (BK20240161, BK20211379), 14th Five-Year Plan of Jiangsu Province medical key disciplines (ZDXK202221), Jiangsu Province clinical key specialty (CZ31202402), 511 Take-off Plan of Jiangsu Province Hospital (JSPH-MA-2020-2), Jiangsu Province Hospital High-Level Talent Cultivation Program (Phase I, CZ0121002010037, CZ0121002010039), Jiangsu Province Hospital Support Plan for Outstanding Young and Middle-aged Talents (YNRCQN005), National Clinical Key Specialty Construction Unit (YWC-ZKJS-2024-04).

Data availability
The datasets generated and analyzed during the current study are available from the corresponding author upon reasonable request.

Declarations

Ethics approval and consent to participate
This study was conducted in accordance with the Declaration of Helsinki and approved by the Ethics Committee of the First Affiliated Hospital with Nanjing Medical University (approval number: 2023-SR-500). Given the retrospective and anonymized nature of this imaging-based study, informed consent for participation was waived by the Ethics Committee. All patient data were anonymized prior to analysis, ensuring confidentiality.

Consent for publication
Not applicable. This manuscript is devoid of any identifiable individual patient data or images that would necessitate consent for publication. All imaging data incorporated were anonymized and utilized exclusively for analytical purposes.

Competing interests
The authors declare no competing interests.

Author details
[1]The First Affiliated Hospital with Nanjing Medical University, 300 Guangzhou Road, Nanjing, Jiangsu 210029, China
[2]School of Basic Medical Sciences of Nanjing Medical University, 101 LongMian Road, Nanjing, Jiangsu 211100, China
[3]Quality Management Office, The Fourth Affiliated Hospital of Nanjing Medical University, Nanjing, Jiangsu 210000, China

Received: 12 March 2025 / Accepted: 14 May 2025
Published online: 30 May 2025

References

1. Lu X, Wei J, Liu Y, Lu Y. Effects of exercise on bone mineral density in middle-aged and older men: A comprehensive meta-analysis. Arch Osteoporos. 2023;18(1):108.
2. Daly RM, Rosengren BE, Alwis G, Ahlborg HG, Sernbo I, Karlsson MK. Gender specific age-related changes in bone density, muscle strength and functional performance in the elderly: a-10 year prospective population-based study. BMC Geriatr. 2013;13:71.
3. Humphrey JA, Woods A, Robinson AHN. The epidemiology and trends in the surgical management of calcaneal fractures in England between 2000 and 2017. Bone Jt J. 2019;101–B(2):140–6.
4. Rupp M, Walter N, Pfeifer C, Lang S, Kerschbaum M, Krutsch W, et al. The incidence of fractures among the adult population of Germany–an analysis from 2009 through 2019. Dtsch Arzteblatt Int. 2021;118(40):665–9.
5. Zhu Y, Li J, Liu S, Chen W, Wang L, Zhang X, et al. Socioeconomic factors and lifestyles influencing the incidence of calcaneal fractures, a National population-based survey in China. J Orthop Surg. 2019;14(1):423.
6. Nam DJ, Kim MS, Kim TH, Kim MW, Kweon SH. Fractures of the distal femur in elderly patients: retrospective analysis of a case series treated with single or double plate. J Orthop Surg. 2022;17(1):55.
7. Xie Y, Zhang L, Xiong Q, Gao Y, Ge W, Tang P. Bench-to-bedside strategies for osteoporotic fracture: from osteoimmunology to mechanosensation. Bone Res. 2019;7:25.
8. Lewis SR, Pritchard MW, Solomon JL, Griffin XL, Bruce J. Surgical versus non-surgical interventions for displaced intra-articular calcaneal fractures. Cochrane Database Syst Rev. 2023;11(11):CD008628.
9. Open reduction and internal. fixation versus nonoperative treatment for closed, displaced, intra-articular fractures of the calcaneus: long-term follow-up from the HeFT randomized controlled trial - PubMed. [cited 2024 Sep 25]. Available from: https://pubmed.ncbi.nlm.nih.gov/34058883/
10. Hu W, Huang C, Zhang Y, Wang X, Jiang Y. A nomogram for predicting post-operative wound complications after open reduction and internal fixation for calcaneal fractures. Int Wound J. 2022;19(8):2163–73.
11. Bremer AK, Kraler L, Frauchiger L, Krause FG, Weber M. Limited open reduction and internal fixation of calcaneal fractures. Foot Ankle Int. 2020;41(1):57–62.
12. Vosoughi AR, Borazjani R, Ghasemi N, Fathi S, Mashhadiagha A, Hoveidaei AH. Different types and epidemiological patterns of calcaneal fractures based on reviewing CT images of 957 fractures. Foot Ankle Surg Off J Eur Soc Foot Ankle Surg. 2022;28(1):88–92.

13. Gougoulias N, McBride D, Maffulli N. Outcomes of management of displaced intra-articular calcaneal fractures. Surg J R Coll Surg Edinb Irel. 2021;19(5):e222–9.
14. Gougoulias N, Khanna A, McBride DJ, Maffulli N. Management of calcaneal fractures: systematic review of randomized trials. Br Med Bull. 2009;92:153–67.
15. Fadle AA, Khalifa AA, Shehata PM, El-Adly W, Osman AE. Extensible lateral approach versus sinus Tarsi approach for Sanders type II and III calcaneal fractures osteosynthesis: a randomized controlled trial of 186 fractures. J Orthop Surg. 2025;20(1):8.
16. The mechanism. reduction technique, and results in fractures of the os calcis - PubMed. [cited 2024 Sep 5]. Available from: https://pubmed.ncbi.nlm.nih.gov/14925322/
17. Burdeaux BD. Reduction of calcaneal fractures by the McReynolds medial approach technique and its experimental basis. Clin Orthop. 1983;(177):87–103.
18. Surgical treatment of displaced intraarticular fractures of the calcaneus. A combined lateral and medial approach - PubMed. [cited 2024 Sep 25]. Available from: https://pubmed.ncbi.nlm.nih.gov/8472473/
19. Deniel C, Guenoun D, Guillin R, Moraux A, Champsaur P, Le Corroller T. Anatomical study of the medial calcaneal nerve using high-resolution ultrasound. Eur Radiol. 2023;33(10):7330–7.
20. Wang J, Qin S, Wang T, Liu J, Wang Z. Comparison of the curative effect of percutaneous reduction with plastic calcaneal forceps combined with medial external fixation in the treatment of Intra-Articular calcaneal fractures. Orthop Surg. 2021;13(8):2344–54.
21. Marchese B, McDonald A, McGowan H. The bifurcation and topography of the posterior tibial artery within the tarsal tunnel. Surg Radiol Anat SRA. 2023;45(5):611–22.
22. Lu M, Cao S, Lu J, Li Y, Li P, Xu J. Three dimensional analysis of factors affecting the prognosis of calcaneal fractures. J Orthop Surg. 2024;19(1):473.
23. Yu Q, Li Z, Li J, Yu Q, Zhang L, Liu D, et al. Calcaneal fracture maps and their determinants. J Orthop Surg. 2022;17(1):39.
24. Zhang H, Lv ML, Liu Y, Sun W, Niu W, Wong DWC, et al. Biomechanical analysis of minimally invasive crossing screw fixation for calcaneal fractures: implications to early weight-bearing rehabilitation. Clin Biomech Bristol Avon. 2020;80:105143.
25. Zheng G, Xia F, Yang S, Cui J. Application of medial column classification in treatment of intra-articular calcaneal fractures. World J Clin Cases. 2020;8(19):4400–9.
26. Shi G, Lin Z, Liu W, Liao X, Xu X, Luo X, et al. 3D mapping of intra-articular calcaneal fractures. Sci Rep. 2023;13(1):8827.
27. Xu H, Hou R, Ju J, Liu Y, Chen L. Articular calcaneal fractures: open or minimally invasive surgery, when the medial wall reduction is obtained percutaneously from the lateral side. Int Orthop. 2021;45(9):2365–73.
28. Guha I, Zhang X, Rajapakse CS, Chang G, Saha PK. Finite element analysis of trabecular bone microstructure using CT imaging and continuum mechanical modeling. Med Phys. 2022;49(6):3886–99.
29. Guo X, Liang X, Jin J, Chen J, Liu J, Qiao Y, et al. Three-dimensional computed tomography mapping of 136 tongue-type calcaneal fractures from a single centre. Ann Transl Med. 2021;9(24):1787–1787.
30. Huang M, Yu B, Li Y, Liao C, Peng J, Guo N. Biomechanics of calcaneus impacted by Talus: a dynamic finite element analysis. Comput Methods Biomech Biomed Engin. 2024;27(7):897–904.
31. Comparison between Percutaneous Screw Fixation and Plate Fixation via Sinus Tarsi Approach for Calcaneal Fractures. An 8-10-Year Follow-up Study - PubMed. [cited 2024 Sep 25]. Available from: https://pubmed.ncbi.nlm.nih.gov/31849195/
32. Kim GB, Park JJ, Park CH. Intra-articular calcaneal fracture treatment with staged medial external fixation. Foot Ankle Int. 2022;43(8):1084–91.
33. Hou J, Zhang N, Chen G, Wang Q, Zhang S, Yang K, et al. Circular external fixator assisted open reduction combined with locking plate fixation for Intra-articular comminuted fractures of the calcaneus. J Foot Ankle Surg Off Publ Am Coll Foot Ankle Surg. 2023;62(3):437–43.
34. Sayyed-Hosseinian SH, Shirazinia M, Arabi H, Aghaee MA, Vahedi E, Bagheri F. Does the postoperative quality of reduction, regardless of the surgical method used in treating a calcaneal fracture, influence patients' functional outcomes? BMC Musculoskelet Disord. 2023;24(1):562.
35. Xu H, Ju J, Hou R, Liu Y, Zhou R, Chen L, et al. Sinus Tarsi approach with percutaneous screw fixation for Intra-Articular calcaneal fractures. J Foot Ankle Surg Off Publ Am Coll Foot Ankle Surg. 2022;61(4):792–7.
36. Shah A, Kothari EA, Young SM, Sanchez T, Sankey T, Murali S, et al. Medial structures at risk during sinus Tarsi approach for fixation of sustentaculum Tali fractures: A cadaveric study. Foot Ankle Orthop. 2022;7(4):24730114211S0093.
37. Kim DI, Kim YS, Han SH. Topography of human ankle joint: focused on posterior tibial artery and tibial nerve. Anat Cell Biol. 2015;48(2):130–7.
38. Warchol Ł, Walocha JA, Mizia E, Bonczar M, Liszka H, Koziej M. Ultrasound-guided topographic anatomy of the medial calcaneal branches of the tibial nerve. Folia Morphol. 2021;80(2):267–74.

Publisher's note